

Modal analysis for nanoplasmonics with nonlocal material properties

Felix Binkowski,¹ Lin Zschiedrich,² Martin Hammerschmidt,² and Sven Burger^{1,2}

¹*Zuse Institute Berlin, Takustraße 7, 14195 Berlin, Germany*

²*JCMwave GmbH, Bolivarallee 22, 14050 Berlin, Germany*

Plasmonic devices with feature sizes of few nanometers exhibit effects which can be described by the nonlocal hydrodynamic Drude model. We demonstrate how to exploit contour integral methods for computing eigenfrequencies and resonant states of such systems. We propose an approach for deriving the modal expansion of relevant physical observables. We use the methods to perform a modal analysis for a metal nanowire. All complex eigenfrequencies in a large frequency range and the corresponding resonant states are computed. We identify those resonant states which are relevant for the extinction cross section of the nanowire.

INTRODUCTION

Nanofabrication technologies allow for a rapid progress in engineering nano-optical devices [1]. Plasmonic resonances are the center of attention for many topical applications exploring new regimes of physics. Examples comprise the demonstration of plasmonic lasers [2], tailoring light emission of nanoantennas [3, 4], probing single molecules and nanoparticles by Raman scattering [5], plasmonic photochemistry [6], and quantum emitters interacting with metal nanoresonators [7].

An adequate description of material dispersion plays an important role for the investigation of light-matter interaction in plasmonic structures [8]. In many cases, the material dispersion can be described by the Drude-Lorentz model or by a rational function fit to measured material data [9, 10]. Such models are based on spatially local interactions between the light and the free electron gas of the plasmonic scatterers [11]. When the scatterers are at the size of a few nanometers, an increasing Fermi pressure of the electron gas leads to additional resonances [12]. Describing these requires a nonlocal material model. Recently, surface plasmon resonance blueshifts have been observed in metal nanoparticles [13, 14] which could be explained [15] using the nonlocal hydrodynamic Drude model (HDM) [16]. This model assumes that the motion of the electron gas behaves as a hydrodynamic flow and allows for the investigation of nonlocal physical effects [17–22].

For the study of physical phenomena in nanoplasmonic systems, a deeper understanding of the effects based on the HDM is required. A modal description is the most instructive approach [23, 24]. In the case of local material models, numerically computed resonant states of plasmonic systems have been successfully used to derive modal expansions [25–28]. However, in the case of the HDM, a coupled system of equations has to be solved [29–31]. To the best of our knowledge, for this system, the computations of eigenfrequencies with corresponding resonant states and modal expansions have not yet been reported.

In this work, we investigate plasmonic resonances

based on the HDM. We present a contour-integral-based framework for a modal analysis. Typical physical observables are sesquilinear forms which involve a complex conjugation of the solution fields. We propose a general approach for the computation of modal sesquilinear quantities. The framework is applied to calculate the eigenfrequencies and corresponding resonant states of a metal nanowire. Furthermore, the modal extinction cross section of the nanowire illuminated by plane waves is computed. This allows to classify the resonant states of the nanowire into states which couple to the light sources and into states which have no contribution to the extinction cross section.

PLASMONIC RESONANCES BASED ON THE HYDRODYNAMIC DRUDE MODEL

The HDM is based on the interaction of a nonlocal polarization current and its resulting electric field. In the frequency domain and for non-magnetic materials, this is described by the coupled system of equations

$$\begin{aligned} \nabla \times \mu_0^{-1} \nabla \times \mathbf{E}(\mathbf{r}, \omega) - \omega^2 \epsilon_{\text{loc}}(\mathbf{r}, \omega) \mathbf{E}(\mathbf{r}, \omega) \\ = i\omega \mathbf{J}_{\text{hd}}(\mathbf{r}, \omega) + i\omega \mathbf{J}(\mathbf{r}, \omega), \end{aligned} \quad (1)$$

$$\begin{aligned} \beta^2 \nabla (\nabla \cdot \mathbf{J}_{\text{hd}}(\mathbf{r}, \omega)) + \omega (\omega + i\gamma) \mathbf{J}_{\text{hd}}(\mathbf{r}, \omega) \\ = i\omega \omega_p^2 \epsilon_0 \mathbf{E}(\mathbf{r}, \omega) \end{aligned} \quad (2)$$

for the electric field $\mathbf{E}(\mathbf{r}, \omega)$ and the nonlocal hydrodynamic current density $\mathbf{J}_{\text{hd}}(\mathbf{r}, \omega)$, where $\mathbf{J}(\mathbf{r}, \omega)$ is a given impressed current density, ω is the frequency, $\epsilon_{\text{loc}}(\mathbf{r}, \omega)$ is the permittivity resulting from the local material response, ϵ_0 is the vacuum permittivity, and μ_0 is the vacuum permeability. The damping constant γ and the plasma frequency ω_p correspond to the local Drude model $\epsilon_d(\omega) = \epsilon_0(\epsilon_\infty - \omega_p^2/(\omega^2 + i\gamma\omega))$, where ϵ_∞ is the relative permittivity at infinity. The factor β relates to the Fermi velocity v_F [16].

The nonlocal material response is caused by $\mathbf{J}_{\text{hd}}(\mathbf{r}, \omega)$, which affects the permittivity function for the free electron gas. If $\beta \rightarrow 0$, then the coupled system simplifies to Maxwell's equations for the local Drude model. For an illustration of the effect of the HDM, a nanowire excited

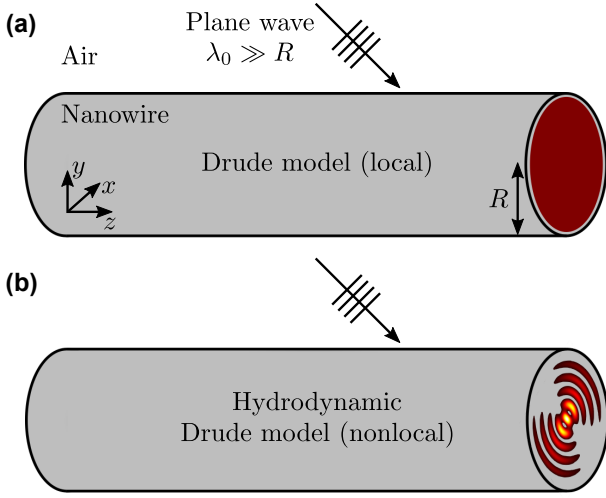


FIG. 1. Schematics of a metal nanowire illuminated by a plane wave of wavelength λ_0 . Electric field intensity sketched on a cut through the nanowire. (a) Constant electric field intensity in case of the local Drude model. (b) Radially oscillating field pattern in case of the nonlocal hydrodynamic Drude model.

by a plane wave is sketched in Fig. 1. While, for the local Drude model, the electric field intensity inside of the nanowire is nearly constant, the electric field pattern is radially oscillating considering the HDM, see Fig. 1(a) and Fig. 1(b), respectively. The reader is referred to [30, 31] for a detailed derivation of Eq. (1) and Eq. (2) including the applied assumptions and approximations.

Physical solutions $\mathbf{E}(\mathbf{r}, \omega_0)$ and $\mathbf{J}_{\text{hd}}(\mathbf{r}, \omega_0)$ of the coupled system can be obtained for real frequencies $\omega_0 \in \mathbb{R}$. The eigenfrequencies are defined as the complex resonance poles $\tilde{\omega}_k \in \mathbb{C}$ of the analytical continuation of $\mathbf{E}(\mathbf{r}, \omega_0)$ and $\mathbf{J}_{\text{hd}}(\mathbf{r}, \omega_0)$ into the complex plane yielding $\mathbf{E}(\mathbf{r}, \omega)$ and $\mathbf{J}_{\text{hd}}(\mathbf{r}, \omega)$, where $\omega \in \mathbb{C}$ [27]. The resonant states, also called eigenmodes, of the coupled system correspond to these eigenfrequencies.

Numerical methods for modal analysis

We apply contour integral methods to numerically solve the eigenproblem corresponding to the coupled system given by Eq. (1) and Eq. (2). Contour integral methods only require the solution of scattering problems. Therefore, the implementation of a scattering solver can be used for the whole presented framework. This is in contrast to standard approaches for solving eigenproblems, such as the Arnoldi method, which requires linearization with auxiliary fields [32]. For the modal expansion of scattering problems, an unconjugated scalar product can be used [28]. In this context, it is an open problem how to deal with the expansion of non-holomorphic quantities, e.g., the extinction cross section. Contour integral methods allow to perform a modal expansion with-

out a scalar product [27].

The eigenmodes of the coupled system are computed using BEYN'S ALGORITHM [33]. This contour integral method requires the definition of an integration path in the complex frequency plane which encloses the eigenfrequencies corresponding to the eigenmodes of interest. The numerical integration along this contour projects vector fields onto the space spanned by these eigenmodes. In this way, an approximate eigenspace is constructed. The eigenfrequencies and the eigenmodes are extracted by a singular-value decomposition (SVD) for this approximate eigenspace. Then, a linear eigenproblem of small dimension is solved.

The coupling of the eigenmodes to specific sources is quantified by applying the Riesz projection expansion (RPE) [27]. This modal expansion approach is also based on contour integration. Instead of projecting random vectors as for BEYN'S ALGORITHM, fields corresponding to physical sources $\mathbf{J}(\mathbf{r}, \omega)$ are applied. The coupled system is therefore solved for $\mathbf{E}(\mathbf{r}, \omega)$ and $\mathbf{J}_{\text{hd}}(\mathbf{r}, \omega)$ at integration points in the complex frequency plane.

Equation (1) and Eq. (2) are spatially discretized with the finite element method (FEM) [34, 35]. The FEM solver JCMSUITE is used to solve scattering problems. Perfectly matched layers (PMLs) are applied to realize outgoing radiation conditions [36]. We write

$$T(\omega)v = f(\omega) \quad (3)$$

for the coupled system given by Eq. (1) and Eq. (2), where $T(\omega) \in \mathbb{C}^{n \times n}$ is the system matrix resulting from the FEM discretization and $v \in \mathbb{C}^n$ is the vector corresponding to $\mathbf{E}(\mathbf{r}, \omega)$ and $\mathbf{J}_{\text{hd}}(\mathbf{r}, \omega)$. The right-hand side $f(\omega)$ corresponds to the impressed current density $\mathbf{J}(\mathbf{r}, \omega)$ and incoming source fields. In this notation, $T(\tilde{\omega}_k)\tilde{v}_k = 0$ holds for an eigenfrequency $\tilde{\omega}_k$ and an eigenmode \tilde{v}_k . Solving $T(\omega)v = f(\omega)$ with $f(\omega) \neq 0$ corresponds to solving a scattering problem.

Modal expansion of sesquilinear quantities

Typical physical quantities are quadratic forms associated with a sesquilinear map $q(v, v^*)$ for solution fields v and their complex conjugates v^* . Examples include the electromagnetic absorption and the electromagnetic energy flux. For two reasons, the construction of a meaningful modal expansion of sesquilinear forms $q(v, v^*)$ is not straightforward. Firstly, the missing orthogonality $q(\tilde{v}_k, \tilde{v}_l^*) \neq 0$ yields cross terms in the expansion. Secondly, the conjugation $v^*(\omega_0)$ renders $q(v(\omega_0), v^*(\omega_0))$ non-holomorphic and the evaluation of this expression for complex eigenfrequencies $\tilde{\omega}_k$ is problematic.

The RPE opens the possibility to derive a modal expansion of sesquilinear quantities with well-defined expansion coefficients. The method is based on an analytical continuation of the sesquilinear form $q(v(\omega_0), v^*(\omega_0))$

from the real axis $\omega_0 \in \mathbb{R}$ into the complex plane $\omega \in \mathbb{C}$. We remark that $v^*(\omega_0)$ is the solution to $T^*(\omega_0)v^*(\omega_0) = f^*(\omega_0)$. The system matrix $T^*(\omega_0)$ and the right-hand side $f^*(\omega_0)$ have analytical continuations, which we denote by $T^\circ(\omega)$ and $f^\circ(\omega)$. Consequently, the analytical continuation of $v^*(\omega_0)$ reads as

$$v^\circ(\omega) = T^\circ(\omega)^{-1} f^\circ(\omega). \quad (4)$$

Finally, this gives the analytical continuation $q(v(\omega), v^\circ(\omega))$ into the complex plane and the modal expansion can be computed.

Note that if a solution of the coupled system given by Eq. (1) and Eq. (2) has a pole in $\omega = \tilde{\omega}_k$, then its complex conjugate has a pole in $\omega = \tilde{\omega}_k^*$. Thus, $q(v(\omega), v^\circ(\omega))$ has poles in $\tilde{\omega}_k$ and also in $\tilde{\omega}_k^*$. This has to be taken into account for the RPE. The calculation of a modal quantity corresponding to a specific $\tilde{\omega}_k$ involves the summation of the Riesz projections for $\tilde{\omega}_k$ and $\tilde{\omega}_k^*$.

As the derivation of $v^\circ(\omega)$ is given formally, we remark, for a better physical understanding, that the complex conjugation of the system matrix and the right-hand side corresponds to solving the coupled system for $\omega = -\omega_0$ with sign-inverted radiation conditions.

RESONANCES OF A NANOWIRE

We consider a specific setup, a cylindrical metal nanowire which has also been investigated in the literature, to study HDM-based effects theoretically [17]. For typical nanoplasmonic applications, a quantity of interest is the extinction cross section. In the following, we first compute eigenfrequencies and eigenmodes of the nanowire. Based on this, we then investigate the extinction cross section in a modal sense, i.e., it is shown which of the eigenmodes scatter and absorb an incoming source field and which of the modes do not interact with the light source.

The investigated sodium nanowire of radius $R = 2$ nm, infinitely extended in z direction, see Fig. 1(a), is described by $\epsilon_\infty = 1$, $\omega_p = 8.65 \times 10^{15} \text{ s}^{-1}$, $\gamma = 0.01 \omega_p$, and $\epsilon_{\text{loc}} = \epsilon_0 \epsilon_\infty$. The system constant β is given by $\beta = \sqrt{3/5} v_F$, where $v_F = 1.07 \times 10^6 \text{ ms}^{-1}$. The nanowire is surrounded by free space with refractive index $n = 1$. The source field is a y polarized plane wave with unit amplitude propagating in x direction. For the FEM discretization, a mesh containing about 2000 triangles with edge lengths from about 0.05 nm to 1 nm is applied. The polynomial degree of the finite elements is set to $p = 3$.

The frequency range $0.4\omega_p < \omega < 1.4\omega_p$ is selected for the modal analysis. To compute eigenmodes \tilde{v}_k using BEYN'S ALGORITHM, an integration contour around this range is defined. The parameters for the algorithm are $N = 160$ integration points, $l = 200$ random vectors, and, for the rank drop detection within the SVD,

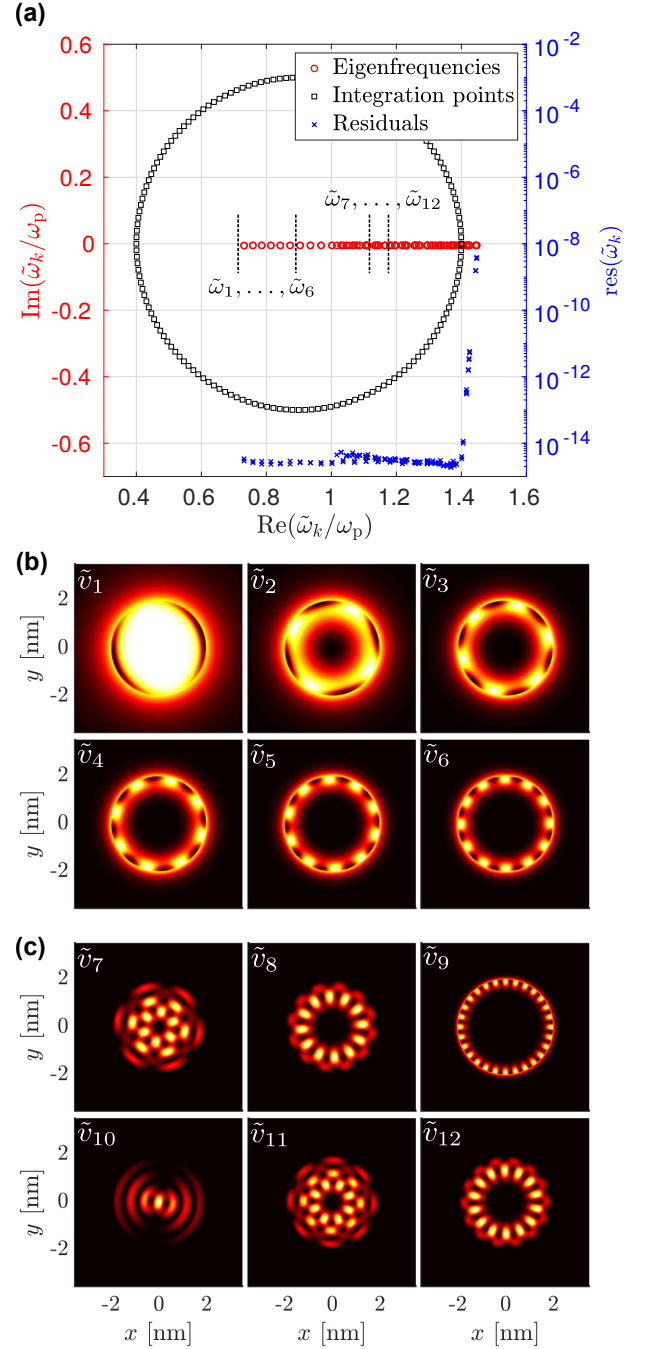


FIG. 2. Eigenfrequencies $\tilde{\omega}_k$ and eigenmodes \tilde{v}_k of the nanowire. (a) Eigenfrequencies, integration points and residuals $\text{res}(\tilde{\omega}_k) = \|T(\tilde{\omega}_k)\tilde{v}_k\|_2 / \|T(\tilde{\omega}_k)\|_F$, where $\|\tilde{v}_k\|_2 = 1$. Inside of the integration contour, 118 eigenfrequencies are located (including multiplicities). (b) Plots (a.u.) of the electric field intensity of an exemplary selection of eigenmodes corresponding to eigenfrequencies below the plasma frequency, $\tilde{\omega}_1 = (0.7313 - 0.0054i)\omega_p$, $\tilde{\omega}_2 = (0.7585 - 0.0050i)\omega_p$, $\tilde{\omega}_3 = (0.7857 - 0.0050i)\omega_p$, $\tilde{\omega}_4 = (0.8138 - 0.0050i)\omega_p$, $\tilde{\omega}_5 = (0.8429 - 0.0050i)\omega_p$, and $\tilde{\omega}_6 = (0.8729 - 0.0050i)\omega_p$. (c) As above, for eigenfrequencies beyond the plasma frequency, $\tilde{\omega}_7 = (1.1341 - 0.0050i)\omega_p$, $\tilde{\omega}_8 = (1.1373 - 0.0050i)\omega_p$, $\tilde{\omega}_9 = (1.1434 - 0.0050i)\omega_p$, $\tilde{\omega}_{10} = (1.1453 - 0.0050i)\omega_p$, $\tilde{\omega}_{11} = (1.1651 - 0.0050i)\omega_p$, and $\tilde{\omega}_{12} = (1.1654 - 0.0050i)\omega_p$. Color scale from zero (black) to one (white).

a tolerance of $\text{tol}_{\text{rank}} = 10^{-8}$ is chosen. The SVD and the solution of the resulting small eigenproblem are performed within MATLAB. We obtain 118 eigenfrequencies inside the integration contour. The imaginary parts of these eigenfrequencies are roughly $\text{Im}(\tilde{\omega}_k) = 0.0050$, except for $\tilde{\omega}_1 = (0.7313 - 0.0054i)\omega_p$. The residuals $\text{res}(\tilde{\omega}_k) = \|T(\tilde{\omega}_k)\tilde{v}_k\|_2 / \|T(\tilde{\omega}_k)\|_F$, where $\|\tilde{v}_k\|_2 = 1$, for eigenfrequencies within the integration contour are smaller than 6×10^{-15} . The residuals for computed eigenfrequencies outside the integration contour increase with the distance to the contour. The integration points, all computed eigenfrequencies, and the residuals are shown in Fig. 2(a). Plots of the electric field intensity of an exemplary selection of eigenmodes corresponding to eigenfrequencies in frequency ranges below and beyond the plasma frequency are shown in Fig. 2(b) and Fig. 2(c), respectively. Note that these eigenfrequencies are semi-simple with an algebraic and geometric multiplicity of two.

Based on the computed spectrum, we investigate the extinction cross section

$$\sigma(\omega_0) = \frac{1}{P_{\text{pw}}} \left[\int_{\delta\Omega} \frac{1}{2} \text{Re}(\mathbf{E}^*(\mathbf{r}, \omega_0) \times \mathbf{H}(\mathbf{r}, \omega_0)) \cdot d\mathbf{S} + \int_{\Omega_{\text{nw}}} \frac{1}{2} \mathbf{E}^*(\mathbf{r}, \omega_0) \cdot \mathbf{J}_{\text{hd}}(\mathbf{r}, \omega_0) dV \right],$$

where the first term is the power flux across the boundary of the entire computational domain, denoted by $\delta\Omega$, and the second term is the energy loss in the domain where the nanowire exists, denoted by Ω_{nw} [30]. The incoming plane wave with real frequencies ω_0 is normalized so that the power flux through the geometrical cross section of the nanowire is $P_{\text{pw}} = 4 \times 10^{-9}$ W. To quantify the coupling of the light source to specific eigenmodes, the RPE is applied. This requires the holomorphic evaluation of sesquilinear quantities from Eq. (4) and yields the modal extinction cross section $\tilde{\sigma}_k(\omega_0)$ corresponding to an eigenfrequency $\tilde{\omega}_k$. The direct solution of the coupled system given by Eq. (1) and Eq. (2) yields the total extinction cross section $\sigma_{\text{tot}}(\omega_0)$.

Firstly, we investigate the modal extinction cross section in a small frequency range including $\tilde{\omega}_7, \dots, \tilde{\omega}_{12}$. Figure 3(a) shows $\tilde{\sigma}_7(\omega_0), \dots, \tilde{\sigma}_{12}(\omega_0)$, and $\sigma_{\text{tot}}(\omega_0)$. The eigenmode \tilde{v}_{10} has a significant contribution to $\sigma_{\text{tot}}(\omega_0)$. The contributions of the eigenmodes $\tilde{v}_7, \tilde{v}_8, \tilde{v}_9, \tilde{v}_{11}$, and \tilde{v}_{12} are negligible.

Secondly, in order to understand why a specific eigenmode couples to the incoming plane wave, a fast Fourier transform of the electric field intensities of the eigenmodes on a circle inside the nanowire is performed. In this way, it is possible to classify the eigenmodes into angular modes with different angular wavenumbers $n_\varphi(\tilde{\omega}_k)$. The decomposition of the plane wave into angular waves using the Jacobi-Anger expansion [34] yields that only eigenmodes with $n_\varphi(\tilde{\omega}_k) = 2$ lead to a relevant coupling. Figure 3(b) shows $n_\varphi(\tilde{\omega}_k)$ for the frequency range

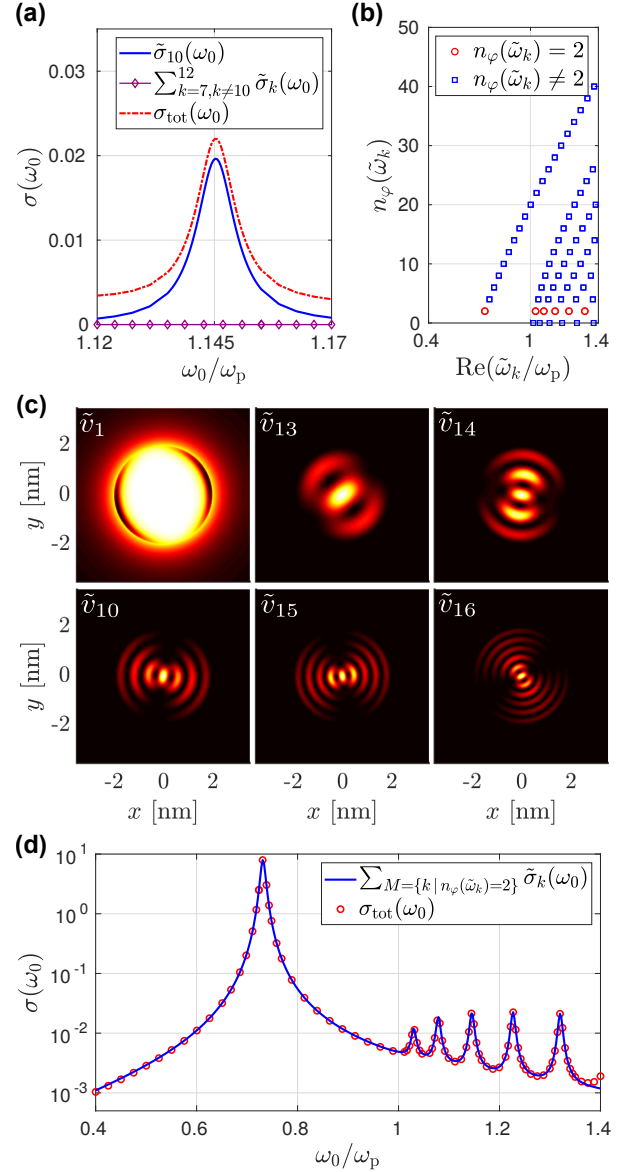


FIG. 3. Modal analysis of the extinction cross section $\sigma(\omega_0)$ of the nanowire. (a) $\sigma(\omega_0)$ for the frequency range $1.12\omega_p < \omega_0 < 1.17\omega_p$. Modal extinction cross section $\tilde{\sigma}_{10}(\omega_0)$ corresponding to the eigenfrequency $\tilde{\omega}_{10} = (1.1453 - 0.0050i)\omega_p$ and the sum $\sum_{k=7, k \neq 10}^{12} \tilde{\sigma}_k(\omega_0)$ corresponding to the remaining eigenfrequencies in the frequency range. Total extinction cross section $\sigma_{\text{tot}}(\omega_0)$ for comparison. (b) Angular wavenumbers $n_\varphi(\tilde{\omega}_k)$ for the eigenfrequencies $\tilde{\omega}_k$ in the frequency range $0.4\omega_p < \text{Re}(\tilde{\omega}_k) < 1.4\omega_p$. (c) Plots (a.u.) of the electric field intensities of the eigenmodes with $n_\varphi(\tilde{\omega}_k) = 2$. Color scale from zero (black) to one (white). (d) Modal expansion of the extinction cross section $\sum_M \tilde{\sigma}_k(\omega_0)$, $M = \{k | n_\varphi(\tilde{\omega}_k) = 2\}$, corresponding to the six eigenfrequencies $\tilde{\omega}_1 = (0.7313 - 0.0054i)\omega_p$, $\tilde{\omega}_{13} = (1.0301 - 0.0050i)\omega_p$, $\tilde{\omega}_{14} = (1.0788 - 0.0050i)\omega_p$, $\tilde{\omega}_{10} = (1.1453 - 0.0050i)\omega_p$, $\tilde{\omega}_{15} = (1.2267 - 0.0050i)\omega_p$, and $\tilde{\omega}_{16} = (1.3202 - 0.0050i)\omega_p$. The total extinction cross section $\sigma_{\text{tot}}(\omega_0)$ is plotted as a reference solution.

$0.4\omega_p < \text{Re}(\tilde{\omega}_k) < 1.4\omega_p$. The field intensities of the six eigenmodes with $n_\varphi(\tilde{\omega}_k) = 2$ are plotted in Fig. 3(c).

Finally, the modal extinction cross sections $\tilde{\sigma}_k(\omega_0)$ for the eigenfrequencies with $n_\varphi(\tilde{\omega}_k) = 2$ are computed. Figure 3(d) shows the sum of the modal extinction cross sections $\sum_M \tilde{\sigma}_k(\omega_0)$, $M = \{k | n_\varphi(\tilde{\omega}_k) = 2\}$. The agreement of this expansion with the total extinction cross section $\sigma_{\text{tot}}(\omega_0)$ demonstrates that the complex scattering behavior of the HDM-based nanowire is governed by few eigenmodes only.

CONCLUSIONS

We investigated the light-matter interaction in nanoplasmonic systems described by the HDM. We presented a contour-integral-based framework for modal analysis, which enables the direct computation of the spectrum of nonlocal material systems. We introduced an approach for the modal expansion of sesquilinear quantities. This opens the possibility to investigate typical physical observables, e.g., the energy flux, the energy absorption, and overlap integrals for extraction efficiencies. Due to the generality of this approach, we expect that it will prove useful also in other fields of physics. Resonant states and the modal extinction cross section of a metal nanowire were calculated. While the spectrum of this system consists of many eigenfrequencies, only a few resonant states have a significant contribution to the extinction cross section. These resonant states were identified and used to expand the quantity of interest.

As demonstrated, nanoplasmonic systems on small length scales exhibit a large number of additional resonant states described by the HDM. A typical feature of these states is their high local field energy concentration. With precisely defined source fields, specific states can be excited. We expect that this will allow for additional degrees of freedom in tailoring light-matter interactions. A modal picture is a prerequisite for the understanding and for the design of corresponding nanoplasmonic devices.

ACKNOWLEDGEMENTS

We acknowledge Philipp-Immanuel Schneider and Fridtjof Betz for fruitful discussions. We acknowledge funding by the Deutsche Forschungsgemeinschaft under Germany's Excellence Strategy - The Berlin Mathematics Research Center MATH+ (EXC-2046/1, project ID: 390685689, AA4-6).

[1] N. C. Lindquist, P. Nagpal, K. M. McPeak, D. J. Norris, and S.-H. Oh, *Rep. Prog. Phys.* **75**, 036501 (2012).

- [2] R. F. Oulton, V. J. Sorger, T. Zentgraf, R.-M. Ma, C. Gladden, L. Dai, G. Bartal, and X. Zhang, *Nature* **461**, 629 (2009).
- [3] A. G. Curto, G. Volpe, T. H. Taminiau, M. P. Kreuzer, R. Quidant, and N. F. van Hulst, *Science* **329**, 930 (2010).
- [4] V. Giannini, A. I. Fernández-Domínguez, S. C. Heck, and S. A. Maier, *Chem. Rev.* **111**, 3888 (2011).
- [5] S. Nie and S. R. Emory, *Science* **275**, 1102 (1997).
- [6] Y. Zhang, S. He, W. Guo, Y. Hu, J. Huang, J. R. Mulcahy, and W. D. Wei, *Chem. Rev.* **118**, 2927 (2018).
- [7] R. Chikkaraddy, B. de Nijs, F. Benz, S. J. Barrow, O. A. Scherman, E. Rosta, A. Demetriadou, P. Fox, O. Hess, and J. J. Baumberg, *Nature* **535**, 127 (2016).
- [8] W. A. Murray and W. L. Barnes, *Adv. Mater.* **19**, 3771 (2007).
- [9] H. S. Sehmi, W. Langbein, and E. A. Muljarov, *Phys. Rev. B* **95**, 115444 (2017).
- [10] M. Garcia-Vergara, G. Demézy, and F. Zolla, *Opt. Lett.* **42**, 1145 (2017).
- [11] P. B. Johnson and R. W. Christy, *Phys. Rev. B* **6**, 4370 (1972).
- [12] S. Raza, S. I. Bozhevolnyi, M. Wubs, and N. A. Mortensen, *J. Phys. Condens. Matter* **27**, 183204 (2015).
- [13] J. A. Scholl, A. L. Koh, and J. A. Dionne, *Nature* **483**, 421 (2012).
- [14] S. Raza, N. Stenger, S. Kadkhodazadeh, S. V. Fischer, N. Kostesha, A.-P. Jauho, A. Burrows, M. Wubs, and N. A. Mortensen, *Nanophotonics*, 131 (2013).
- [15] T. Christensen, W. Yan, S. Raza, A.-P. Jauho, N. A. Mortensen, and M. Wubs, *ACS Nano* **8**, 1745 (2014).
- [16] A. D. Boardman, *Electromagnetic Surface Modes. Hydrodynamic theory of plasmon-polaritons on plane surfaces* (Wiley, New York, 1982).
- [17] R. Rupp, *Opt. Commun.* **190**, 205 (2001).
- [18] S. Palomba, L. Novotny, and R. Palmer, *Opt. Commun.* **281**, 480 (2008).
- [19] F. J. Garca de Abajo, *J. Phys. Chem. C* **112**, 17983 (2008).
- [20] F. Intravaia and K. Busch, *Phys. Rev. A* **91**, 053836 (2015).
- [21] G. Toscano, J. Straubel, A. Kwiatkowski, C. Rockstuhl, F. Evers, N. A. Mortensen, and M. Wubs, *Nat. Commun.* **6**, 7132 (2015).
- [22] M. Moefert, T. Kiel, T. Sproll, F. Intravaia, and K. Busch, *Phys. Rev. B* **97**, 075431 (2018).
- [23] P. T. Kristensen and S. Hughes, *ACS Photonics* **1**, 2 (2014).
- [24] P. Lalanne, W. Yan, K. Vynck, C. Sauvan, and J.-P. Hugonin, *Laser Photonics Rev.* **12**, 1700113 (2018).
- [25] C. Sauvan, J.-P. Hugonin, I. S. Maksymov, and P. Lalanne, *Phys. Rev. Lett.* **110**, 237401 (2013).
- [26] M. Kamandar Dezfouli, R. Gordon, and S. Hughes, *Phys. Rev. A* **95**, 013846 (2017).
- [27] L. Zschiedrich, F. Binkowski, N. Nikolay, O. Benson, G. Kewes, and S. Burger, *Phys. Rev. A* **98**, 043806 (2018).
- [28] W. Yan, R. Faggiani, and P. Lalanne, *Phys. Rev. B* **97**, 205422 (2018).
- [29] J. M. McMahon, S. K. Gray, and G. C. Schatz, *Phys. Rev. Lett.* **103**, 097403 (2009).
- [30] K. R. Hiremath, L. Zschiedrich, and F. Schmidt, *J. Comp. Phys.* **231**, 5890 (2012).

- [31] G. Toscano, S. Raza, A.-P. Jauho, N. A. Mortensen, and M. Wubs, *Opt. Express* **20**, 4176 (2012).
- [32] Y. Brûlé, B. Gralak, and G. Demésy, *J. Opt. Soc. Am. B* **33**, 691 (2016).
- [33] W.-J. Beyn, *Linear Algebra Its Appl.* **436**, 3839 (2012).
- [34] P. Monk, *Finite element methods for Maxwell's equations* (Clarendon Press, Oxford, 2003).
- [35] M. Weiser, *Inside Finite Elements* (De Gruyter, Berlin, 2016).
- [36] J.-P. Berenger, *J. Comput. Phys.* **114**, 185 (1994).